Assessment of the ultraviolet radiation field in ocean waters from space-based measurements and full radiative-transfer calculations

Alexander P. Vasilkov, Jay R. Herman, Ziauddin Ahmad, Mati Kahru, and B. Greg Mitchell

Quantitative assessment of the UV effects on aquatic ecosystems requires an estimate of the in-water radiation field. Actual ocean UV reflectances are needed for improving the total ozone retrievals from the total ozone mapping spectrometer (TOMS) and the ozone monitoring instrument (OMI) flown on NASA's Aura satellite. The estimate of underwater UV radiation can be done on the basis of measurements from the TOMS/OMI and full models of radiative transfer (RT) in the atmosphere–ocean system. The Hydrolight code, modified for extension to the UV, is used for the generation of look-up tables for in-water irradiances. A look-up table for surface radiances generated with a full RT code is input for the Hydrolight simulations. A model of seawater inherent optical properties (IOPs) is an extension of the Case 1 water model to the UV. A new element of the IOP model is parameterization of particulate matter absorption based on recent *in situ* data. A chlorophyll product from ocean color sensors is input for the IOP model. Verification of the in-water computational scheme shows that the calculated diffuse attenuation coefficient K_d is in good agreement with the measured K_d.

OCIS codes: 010.1290, 010.4450, 280.0280.

1. Introduction

Increased levels of biologically harmful UV radiation resulting from the depletion of Earth's ozone layer have been shown to affect aquatic ecosystems. One important effect of enhanced levels of UVB radiation is a reduction in the productivity of phytoplankton caused by the inhibition of photosynthesis due to damage to the photosynthetic apparatus. Enhanced UVB radiation could also affect the photochemical production of carbonyl sulfide in seawater, thereby augmenting the greenhouse effect and affecting other long-term global biogeochemical cycles. Photochemical degradation of oceanic-dissolved organic matter associated with changes in UV radiation flux may affect carbon cycling. A comprehensive overview of the effects of UV radiation on marine ecosystems has been published recently.[1]

The variability of ocean reflectance in the UV can affect measurements by satellite instruments such as the total ozone mapping spectrometer (TOMS) flown on Nimbus-7 and Meteor-3 satellites or the ozone monitoring instrument (OMI) flown on the Aura satellite. Currently the TOMS total column ozone and aerosol products are derived by using the monthly global database of minimum Lambert equivalent surface reflectivity derived from the Nimbus-7/TOMS measurements.[2] An actual estimate of the ocean reflectance in the UV can improve the retrieval of total column ozone and aerosol from the TOMS and OMI observations.

The quantitative assessment of UV effects on aquatic organisms and the ocean UV reflectance requires an estimate of the in-water radiation field.[3] There are two basic requirements for radiative-transfer (RT) schemes for such estimates of the underwater radiation field. The RT scheme should be fast enough for one to compute the spectral UV penetration into the ocean on a global scale in a reasonable time. The RT scheme should have sufficient

A. P. Vasilkov (alexander_vassilkov@ssaihq.com) is with the Science Systems and Applications, Inc., 10210 Greenbelt Road, Lanham, Maryland 20706. J. R. Herman is with NASA Goddard Space Flight Center, Code 916, Greenbelt, Maryland 20771. Z. Ahmad is with Science and Data Systems, Inc., Silver Spring, Maryland 20906. M. Kahru and B. G. Mitchell are with the Scripps Institution of Oceanography, University of California San Diego, La Jolla, California 92093.

Received 25 June 2004; revised manuscript received 14 October 2004; accepted 29 October 2004.

0003-6935/05/142863-07$15.00/0

accuracy at biologically significant optical depths. An estimate of underwater irradiance on a global scale has been made with satellite measurements from TOMS and sea-viewing wide field-of-view sensor (SeaWiFS) instruments and approximate RT models in the atmosphere–ocean system.[4] Given small ocean albedo in the UV, the atmospheric and oceanic RT problems were treated separately in this paper. Radiative-transfer calculations in the ocean were carried out with the quasi-single-scattering approximation (QSSA). The QSSA is a computationally rapid model allowing the estimate of UV penetration into ocean waters on a global scale. However, the QSSA model accuracy is not sufficient for all cases. To improve in-water calculation accuracy and still keep high calculation speeds, we propose use of a look-up table for downward irradiance precomputed with a full RT model, such as Hydrolight,[5] with our extensions for UV ocean optical properties into the 290–400-nm wavelength range.

Solar direct and diffuse radiances at the ocean surface are input for the UV-extended Hydrolight. The radiances are calculated with look-up tables generated with full RT codes.[6,7] An essential component of the in-water RT model is a model of seawater inherent optical properties (IOPs) in the UV spectral region. Unlike models of IOPs in the visible, models of IOPs in the UV are still evolving. We propose an IOP model that is an extension of the Case 1 water model to the UV spectral region. Pure-water absorption is interpolated between experimental data sets available in the literature. A new element of the IOP model is parameterization of particulate-matter absorption in the UV based on recent *in situ* data. The IOP model is verified by comparing the measured and computed values of the diffuse attenuation coefficient.

2. Model of Seawater Inherent Optical Properties

The UV-IOP model used here is similar to one proposed in our previous paper[4] and is an extension of the Case 1 water model to the UV spectral region (290–400 nm). The model was updated by specifying the chlorophyll-specific absorption coefficient as a function of chlorophyll concentration. This parameterization of particulate-matter absorption in the UV is based on recent *in situ* data collected in the framework of the California Cooperative Oceanic Fisheries Investigations (CalCOFI).

The total IOPs are the sums of the IOP of pure seawater and scattering and absorbing water constituents:

$$a(\lambda) = a_w(\lambda) + a_p(\lambda) + a_{\mathrm{CDOM}}(\lambda),$$

$$b(\lambda) = b_w(\lambda) + b_p(\lambda), \tag{1}$$

where a is the absorption coefficient; b is the scattering coefficient; subscripts w, p, and CDOM denote pure water, particulate matter, and colored dissolved organic matter, respectively. We neglect possible absorption by sea salts mostly because of the lack of data on sea-salt absorbance in the literature. At present there are no consensus values for the pure-water absorption coefficient in the UV. According to recent findings[8,9] the pure-water absorption coefficient is significantly lower than previous values.[10] A comparison of available data sets on the pure-water absorption coefficient in the UV along with interpolation between them is given in our paper.[11] The comparison shows a significant difference between the available data sets. In this study we use interpolation between data given in Refs. 8 and 12 as recommended in Ref. 13. Note that a model of ocean Raman scattering[14] agrees well with the observations of the global ozone monitoring experiment only when the interpolated values of the pure-water absorption coefficient are used. The pure-seawater scattering coefficient is accepted from Ref. 10.

The CDOM absorption coefficient and the particulate-matter scattering coefficient are parameterized in the conventional form:

$$a_{\mathrm{CDOM}}(\lambda) = a_0 \exp[-S(\lambda - \lambda_0)],$$

$$b_p(\lambda) = b_0(\lambda/\lambda_0)^{-m}. \tag{2}$$

We adopt an average value of the CDOM spectral slope for the UV spectral region, $S = 0.017\ \mathrm{nm}^{-1}$, as recommended in Ref. 15 and an average estimate of the parameter $m = 1$ as recommended in Ref. 16. The particulate-matter absorption is expressed through a chlorophyll-a concentration C and a chlorophyll-specific absorption coefficient, $a_p(\lambda) = Ca_p^*(C, \lambda)$. Parameterization of the chlorophyll-specific absorption coefficient in the UV is similar to the one developed in the visible,[17] $a_p^*(C, \lambda) = A(\lambda)C^{-B(\lambda)}$. Coefficients $A(\lambda)$ and $B(\lambda)$ were determined from CalCOFI data sets.[11,18] Values of these coefficients along with the correlation coefficient are in Table 1, assuming that the chlorophyll concentration is expressed in milligrams per cubic meter. Note that the correlation coefficient diminishes with decreasing wavelength. This suggests higher variability of the particulate matter absorption coefficient in the UVB than in the UVA. Coefficients $A(\lambda)$ and $B(\lambda)$ were extrapolated to shorter wavelengths, as short as 290 nm. Accuracy in the extrapolation does not play a significant role because of the extremely low values of solar surface flux in the spectral range of 290–300 nm, mostly absorbed by ozone in the atmosphere. A comparison of this parameterization of particulate-matter absorption developed on the basis of data sets from the CalCOFI with simplified parameterization used in Ref. 4 showed the CalCOFI parameterization results in noticeably higher values of the particulate-matter absorption coefficient, particularly for low chlorophyll concentration.[11] This may be explained by a limited data set of *in situ* measurements used for the simplified parameterization.[4]

The IOP model contains three input quantities: a_0, b_0, and C. To reduce the number of input parameters,

Table 1. Regression Coefficients $A(\lambda)$ and $B(\lambda)$ and Correlation Coefficient r

Wavelength (nm)	A	B	r	Wavelength (nm)	A	B	r
300.0	0.1023	0.0983	0.724	350.0	0.0709	0.153	0.804
302.0	0.1022	0.0989	0.723	352.0	0.0681	0.154	0.809
304.0	0.1016	0.0994	0.721	354.0	0.0656	0.155	0.814
306.0	0.1007	0.100	0.718	356.0	0.0634	0.156	0.818
308.0	0.0997	0.101	0.716	358.0	0.0617	0.158	0.822
310.0	0.0986	0.103	0.713	360.0	0.0604	0.160	0.826
312.0	0.0977	0.105	0.711	362.0	0.0595	0.162	0.830
314.0	0.0970	0.108	0.710	364.0	0.0590	0.164	0.834
316.0	0.0965	0.112	0.711	366.0	0.0586	0.167	0.838
318.0	0.0961	0.116	0.713	368.0	0.0583	0.169	0.842
320.0	0.0958	0.120	0.717	370.0	0.0580	0.172	0.847
322.0	0.0955	0.124	0.721	372.0	0.0577	0.174	0.851
324.0	0.0951	0.128	0.726	374.0	0.0572	0.176	0.856
326.0	0.0944	0.132	0.731	376.0	0.0567	0.178	0.860
328.0	0.0935	0.135	0.736	378.0	0.0561	0.180	0.865
330.0	0.0924	0.137	0.740	380.0	0.0556	0.182	0.869
332.0	0.0911	0.140	0.745	382.0	0.0551	0.184	0.874
334.0	0.0896	0.142	0.750	384.0	0.0546	0.186	0.878
336.0	0.0880	0.143	0.756	386.0	0.0541	0.188	0.882
338.0	0.0861	0.145	0.763	388.0	0.0537	0.189	0.886
340.0	0.0841	0.147	0.769	390.0	0.0532	0.191	0.890
342.0	0.0818	0.149	0.777	392.0	0.0527	0.192	0.893
344.0	0.0793	0.150	0.784	394.0	0.0523	0.193	0.896
346.0	0.0766	0.151	0.791	396.0	0.0520	0.194	0.899
348.0	0.0738	0.152	0.798	398.0	0.0519	0.196	0.903
				400.0	0.0520	0.198	0.907

the Case 1 water model[16] is assumed. According to the model the CDOM absorption at 440 nm is 20% of the total absorption of pure seawater and particulate-matter pigments. This assumption determines the important parameter a_0. According to the Case 1 water model, the particulate total scattering coefficient is a function of chlorophyll concentration. A value of the particulate total scattering coefficient at 550 nm is approximated as $b_0 = 0.416C^{0.766}$ (see Refs. 19 and 20). Thus all the input parameters are functions of only one physical input quantity—the chlorophyll concentration that comes from satellite ocean color measurements.

In the simulations we used several phase-scattering functions. One of them is the Petzold average-particle phase function most commonly used in numerical RT studies.[5] Others were the Fournier–Forand (FF) phase functions with different values of the anisotropy coefficient.[21]

3. In-Water Irradiance Look-Up Table

Ultraviolet irradiance in the ocean is calculated by using a look-up table generated with the UV-extended Hydrolight and look-up tables for surface radiances. Details of the surface look-up-table generation can be found in Ref. 22. Briefly the surface look-up tables were generated by using the vector Gauss–Seidel iteration code[6] for clear skies and the discrete ordinates radiative transfer (DISORT) code[7] for cloudy conditions. The Gauss–Seidel iteration code is capable of accounting for a rough ocean surface. Approximate coupling of RT in the atmosphere–ocean system is based on assumed diffuse reflectance of the ocean. The ozone amounts were varied from 125 to 575 Dobson units (DU) to cover the global range of the total column ozone.

Our UV-extended model of seawater IOP was implemented in the 4.06 version of Hydrolight. The Petzold average-particle phase function with a backscatter fraction of 0.018 and the FF phase function with a backscatter fraction as low as 0.003 were used in the computations. Interpolation between irradiances calculated for these two phase functions would allow computations for most oceanic conditions provided information about a phase function is available. The RT computations were conducted for vertically homogeneous waters. Based on these assumptions, look-up tables for in-water downward and upward irradiances were generated for chlorophyll concentrations that varied from 0.01 to 5 mg/m^3. The simulations were carried out in the UV region of 290–400 nm and for solar zenith angles (SZAs) ranging from 0 to 80 deg. The spectral resolution, which was equal to 2 nm in the UVB and 5 nm in the UVA, is sufficient to allow accurate convolution of UV fluxes with the action spectra available.[1]

Figures 1 and 2 illustrate a few dependences calculated with the look-up tables for clear skies. Figure 1 shows the total ozone dependence of downward irradiance at a depth of 4 m. Irradiance was calculated for different SZAs and wavelengths. The total ozone dependence is close to linear when the irradiance is

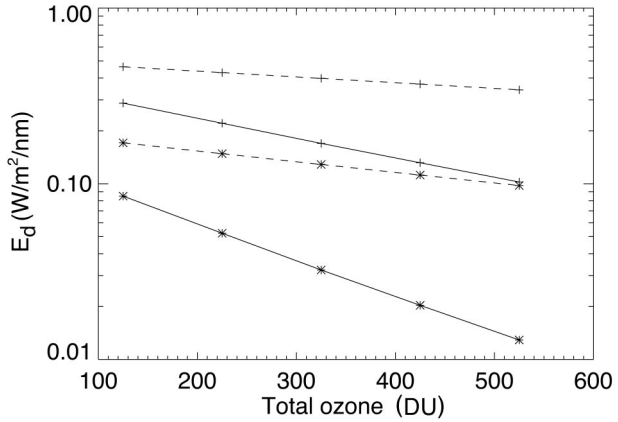

Fig. 1. Downward irradiance at a depth of 4 m calculated for different wavelengths and SZAs: solid lines, 310 nm; dashed lines, 320 nm; plus signs, SZA = 15°; asterisks, SZA = 60°.

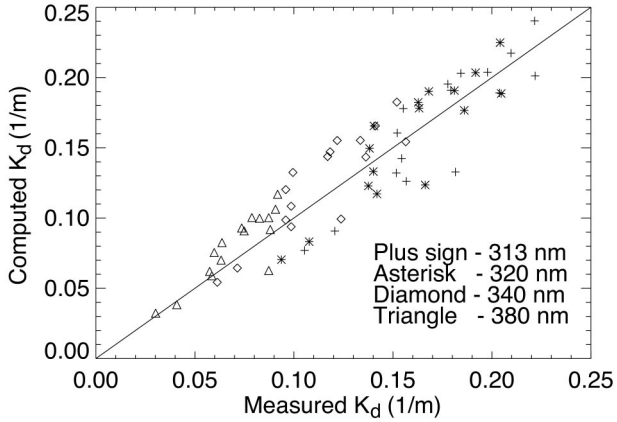

Fig. 3. Comparison of the measured and calculated K_d averaged over a 10-m layer.

plotted on the logarithmic scale. The slope of this linear dependence is reduced as the SZA decreases. The slope reduction approximately follows the air mass change with the SZA.

Figure 2 shows the wavelength dependence of the penetration depth defined as a depth at which the total downward irradiance is reduced to 10% of its surface value. The penetration depth was calculated for different SZAs and chlorophyll concentrations. The chlorophyll dependence of the penetration depth is obvious: It closely follows the total absorption of seawater because the diffuse attenuation coefficient is mostly determined by seawater absorption while scattering plays an insignificant role because of the strong anisotropy of seawater scattering. The SZA dependence of the penetration depth is less obvious. Variations of the SZA cause a change in the angular distribution of light incident on the ocean surface. The change in the angular distribution of light leads to a change in the diffuse attenuation coefficient because the irradiance attenuation depends on the angular distribution of light penetrating into the ocean.[23] This dependence is relatively weak; however, it exists.

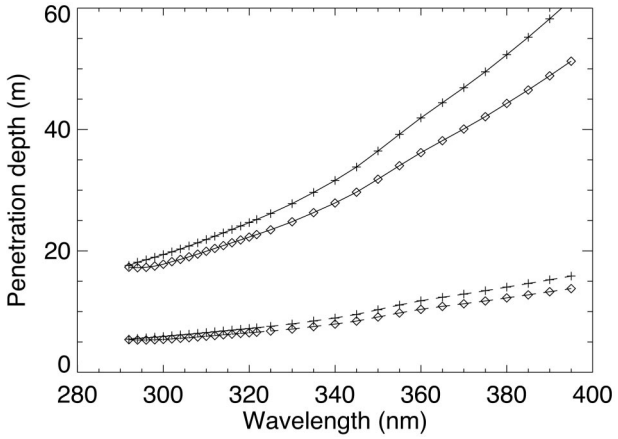

Fig. 2. Penetration depth calculated for different chlorophyll concentrations and SZAs: solid curves, $C = 0.1$ mg/m^3; dashed curves, $C = 1.0$ mg/m^3; plus signs, SZA = 15°; diamonds, SZA = 60°.

4. Verification of the Inherent Optical Property Model

We assume that our full RT models produce acceptable if not negligible errors in calculated underwater irradiances provided the IOPs are known. The accuracy of the in-water radiation field is mostly limited by errors in the IOP model. We verified the IOP model by a comparison of the calculated and measured diffuse attenuation coefficients K_d. In general K_d depends on the angular structure of the light field and thus on depth (even in a homogeneous ocean).[23] However, K_d depends mainly on the seawater IOP.[24] The diffuse attenuation coefficient does not depend on the absolute values of surface irradiance. Therefore a comparison of the calculated and measured K_d is suitable for verification of the IOP model. To simplify the comparison, we computed the diffuse attenuation coefficient for clear-sky conditions only, even though some measurements were done for partial-cloud conditions. A single low-latitude vertical profile of ozone with a total column amount of 325 DU was assumed in the computations.

In situ data used in the comparisons are from measurements taken in the framework of the Aerosol Characterization Experiment (ACE)-Asia experiment in the Pacific Ocean. The measurements cover the time period from 16 April 2001 to 17 March 2001, while the spatial coverage of the data is from 25 °N to 39 °N and 177 °W to 178 °E. The underwater measurements were performed with the MER PRR-800 high-resolution, underwater profiling reflectance radiometer. The data set includes profile measurements of downward irradiance E_d, upward irradiance E_u, and upward radiance L_u at 17 wavelengths ranging from 313 to 710 nm. (The UV wavelengths are 313, 320, 340, 380, and 395 nm.) The diffuse attenuation coefficient K_d was calculated from the downward irradiance. Measurements of surface chlorophyll concentration were also available for the same cruise.

Figure 3 shows a comparison of the measured and

computed diffuse attenuation coefficients averaged over a layer of 6–16 m. In computations the look-up table generated for the Petzold phase function is used. The comparison is done for the cruise stations with chlorophyll concentrations of less than 0.7 mg/m^3 to ensure the validity of assumptions of the Case 1 water model. Data from station 9 were excluded from the comparison because of excessively large differences between the measured and the calculated vertical profiles of K_d. The correlation coefficient is equal to 0.89 for wavelengths of 313, 320, and 340 nm. Its value of 0.87 is slightly lower for a wavelength of 380 nm. The relative rms error for all the cruise stations is ~20%. The computations were conducted for clear-sky conditions. The presence of aerosols and/or clouds changes the angular distribution of incident radiation and slightly changes the estimated value of K_d. The scatter of the calculated K_d around the 1:1 line in Fig. 3 may be partially attributed to changes in the ratio of direct to diffuse radiation caused by aerosols and cloudiness. Note that there is no obvious bias between the measured and the calculated K_d, suggesting that the IOP model reasonably reflects the observed absorption and scattering in the ocean, particularly taking into account that the accuracy of the current optical measurements of the individual IOPs is not better than 10%.

Note that excluding the absorption by CDOM in the IOP model results in a substantial reduction of K_d, suggesting that the CDOM absorption is an essential factor affecting the UV penetration into the ocean.[25] The CDOM absorption in the UV is not negligible even for the clearest waters with chlorophyll concentrations lower than 0.1 mg/m^3. The Case 1 water model assumes that there are two parts of CDOM absorption: The least background absorption by CDOM that is independent of chlorophyll and major absorption entirely correlated with chlorophyll. However, *in situ* data collected in the CALCOFI cruises show that the correlation between CDOM absorption in the UV and chlorophyll concentration may not be high even in Case 1 waters.[18] This fact shows a need for further improvements to the IOP model in the UV.

It is well known that a phase-scattering function substantially affects the seawater reflectance.[26] At the same time its effects on the diffuse attenuation coefficient are noticeably weaker. Figure 4 shows a percentage difference in the irradiance reflectances, $R = E_u/E_d$, and diffuse attenuation coefficients K_d computed with the Petzold and FF phase functions for two wavelengths, 310 and 380 nm. The difference is defined as $\Delta R = R(\mathrm{FF})/R(\mathrm{Petzold})$-1, and it is similar for K_d. The difference in K_d at 380 nm is within 20% for chlorophyll concentrations lower than 1 mg/m^3. However, the difference in the diffuse reflectances at 380 nm is significantly higher, as high as 65% for the same chlorophyll concentration range. The differences at 310 nm are noticeably lower than at 380 nm. This fact is explained by higher absorption at 310 nm than at 380 nm; thus the effects of scattering are reduced.

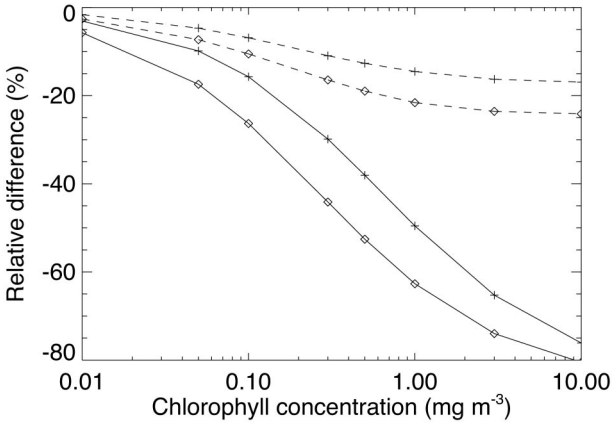

Fig. 4. Percentage difference in the diffuse reflectance (solid curves) and the diffuse attenuation coefficient (dashed curves), as computed with the Petzold phase function and the FF phase function with a backscatter ratio of 0.003 (see the text for a definition of the difference): plus signs, 310 nm; diamonds, 380 nm.

We have attempted to compare the measured and the calculated irradiance reflectance $R = E_u/E_d$ at different depths.[25] The calculations were carried out for the Petzold phase function. The comparison of the reflectance just beneath the sea surface showed a substantial bias: The computed reflectance was systematically higher than the measured reflectance. The *in situ* data were actually extrapolated to zero depth. Note that the *in situ* data extrapolated to a depth of 1–3 m were in better agreement with the computed reflectance. However, the differences between the measured and the calculated values were still significant. Figure 5 shows a comparison of the reflectance measured at a depth of 2 m with the reflectance calculated for the Petzold and FF phase functions. The FF phase function has a backscatter fraction of 0.003. The comparison is for a wavelength of 380 nm where the effect of a phase function is more

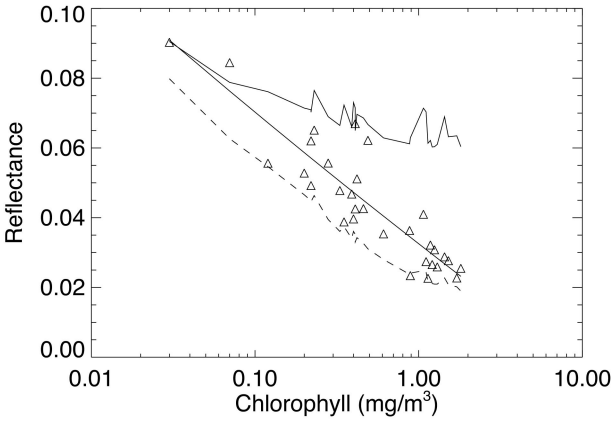

Fig. 5. Comparison of the measured reflectance at 380 nm with the reflectance computed for the Petzold (solid curve) and the FF (dashed curve) phase functions. A least-squares fit to the measured reflectance is shown by the solid line.

pronounced than for shorter wavelengths. Calculations were done for SZAs of *in situ* measurements. Spikes seen on the curves are caused by variations of the SZA because the diffuse reflectance depends on the SZA. A least-squares fit to the measured reflectance is also shown in Fig. 5. It is known that the backscatter ratio depends on the chlorophyll concentration ranging from 0.02 for oligotrophic waters with extremely low chlorophyll to 0.002 for eutrophic waters with extremely high chlorophyll.[16] A comparison of the measured reflectance with the calculated reflectance shows a better agreement for the Petzold function when chlorophyll concentration is low and for the FF phase function when chlorophyll concentration is high. However, the diffuse attenuation coefficients computed for the FF phase function appears to be systematically lower than the measured diffuse attenuation coefficient. The reasons for inconsistency between the reflectance and the diffuse attenuation coefficient are not completely understood. The good agreement between the measured and the computed diffuse attenuation coefficients suggests using the Petzold phase function in the assessment of UV penetration into the ocean.

5. Model Application

The entire computational scheme was applied for global mapping in-water irradiances and penetration depths.[22] The penetration depth is defined as a depth at which total downward irradiance is reduced to 10% of its surface value. The penetration depth was computed by using the generated look-up tables, SeaWiFS monthly chlorophyll concentrations, and TOMS reflectivity as inputs for the model. The penetration depths are determined by the spatial distribution of chlorophyll concentration as expected.[4] The effects of the cloudiness structure and the total ozone distribution cannot be distinguished clearly. This fact proves additionally that the diffuse attenuation coefficient can be used for verification of the IOP model.

The 10% penetration depths for the UVB and the DNA dose were also mapped in our previous paper.[4] The penetration depths in this paper were calculated by using the computationally efficient but not exact QSSA model. The QSSA accuracy was estimated by a comparison of K_d calculated by the QSSA model with K_d exactly calculated with the UV-extended Hydrolight.[27] The above-described IOP model was used in both RT models. The calculations were done for a variety of environment and geometrical conditions of *in situ* measurements in the ACE-Asia experiment. The comparison of K_d showed that the QSSA model underestimates K_d by 20% on average.[27]

An underestimation of K_d by the QSSA model could lead to an approximately 20% overestimation of the penetration depths mapped in Ref. 4. However, computation of the penetration depth in that paper was done with the pure-water absorption coefficient adopted from Ref. 10. These values of the pure-water absorption coefficient in the UV were significantly larger than the values accepted in the present paper. The resulting overestimation of the penetration depth due to the QSSA model was to some extent canceled by using the larger values of the pure-water absorption coefficient.

6. Conclusions

A model for assessing the UV radiation field in the ocean on a global scale has been developed. The model simulations of underwater UV radiation has been performed on the basis of satellite measurements from the TOMS and SeaWiFS and look-up tables generated with accurate models of radiative transfer in the atmosphere–ocean system. The look-up table for in-water downward irradiance was generated with the UV-extended Hydrolight code for the 290–400-nm wavelength range and look-up tables for surface radiances. An essential component of the in-water RT model is a model of seawater inherent optical properties. The IOP model is an extension of the Case 1 water model to the UV spectral region. Pure-water absorption is interpolated between experimental data sets available in the literature. A new element of the IOP model is parameterization of particulate-matter absorption in the UV based on recent *in situ* data. The comparison between the measured and the computed K_d proves that the IOP model is reasonably adequate in the UV. The K_d calculated with the UV-extended Hydrolight is in rather good agreement with the measured K_d. The relative rms error for all the cruise stations is ~20%. The error may be partially attributed to changes in the angular distribution of surface radiation caused by aerosols and cloudiness. Excluding absorption by colored dissolved organic matter in the IOP model results in a substantial reduction in K_d, thus suggesting that the CDOM absorption is an essential factor affecting the UV penetration into the ocean. It has been shown that the QSSA model underestimates K_d by 20% on average. An important conclusion is that we are now able to model ocean UV irradiances and IOP properties with accuracies approaching those visible regions and in agreement with experimental *in situ* data.

A. P. Vasilkov gratefully acknowledges support from NASA contract NAS5-00220.

References

1. S. de More, S. Demers, and M. Vernet, eds., *The Effects of UV Radiation in the Marine Environment* (Cambridge University, Cambridge, UK, 2000).
2. J. R. Herman and E. Celarier, "Earth surface reflectivity climatology at 340 to 380 nm from TOMS data," J. Geophys. Res. **102,** 28003–28011 (1997).
3. K. Stamnes, "Ultraviolet and visible radiation in the atmosphere–ocean system: a tutorial review of modeling capabilities," Opt. Eng. **41,** 3008–3018 (2002).
4. A. P. Vasilkov, N. Krotkov, J. R. Herman, C. McClain, K. Arrigo, and W. Robinson, "Global mapping of underwater UV irradiance and DNA-weighted exposures using TOMS and SeaWiFS data products," J. Geophys. Res. **106,** 27205–27219 (2001).
5. C. D. Mobley, *Light and Water: Radiative Transfer in Natural Waters* (Academic, San Diego, Calif., 1994).

6. Z. Ahmad and R. S. Fraser, "An iterative radiative transfer code for ocean–atmosphere systems," J. Atmos. Sci. **39,** 656–665 (1982).
7. K. Stamnes, S.-C. Tsay, W. Wiscombe, and K. Jayaweera, "Numerically stable algorithm for discrete ordinate method radiative transfer in multiple scattering and emitting layered media," Appl. Opt. **27,** 2502–2509 (1988).
8. R. M. Pope and E. S. Fry, "Absorption spectrum (380–700 nm) of pure water. II. Integrating cavity measurements," Appl. Opt. **36,** 8710–8723 (1997).
9. F. M. Sogandares and E. S. Fry, "Absorption spectrum (340–700 nm) of pure water. I. Photothermal measurements," Appl. Opt. **36,** 8710–8723 (1997).
10. R. C. Smith and K. C. Baker, "Optical properties of the clearest natural waters," Appl. Opt. **20,** 177–186 (1981).
11. A. P. Vasilkov, J. Herman, N. A. Krotkov, M. Kahru, B. G. Mitchell, and C. Hsu, "Problems in assessment of the UV penetration into natural waters from space-based measurements," Opt. Eng. **41,** 3019–3027 (2002).
12. T. I. Quickenden and J. A. Irvin, "The ultraviolet absorption spectrum of liquid water," J. Chem. Phys. **72,** 4416–4428 (1980).
13. E. S. Fry, "Visible and near ultraviolet absorption spectrum of liquid water," Appl. Opt. **39,** 2743–2744 (2000).
14. A. P. Vasilkov, J. Joiner, J. Gleason, and P. K. Bhartia, "Ocean Raman scattering in satellite backscatter UV measurements," Geophys. Res. Lett. **29**(17), 1837, doi:10.1029/2002GL014955 (2002).
15. O. V. Kopelevich, S. V. Lutsarev, and V. V. Rodionov, "Light spectral absorption by yellow substance of ocean water," Oceanology **29,** 409–414 (1989).
16. A. Morel, "Optical modeling of the upper ocean in relation to its biogeneous matter content (Case I waters)," J. Geophys. Res. **93,** 10749–10768 (1988).
17. A. Bricaud, M. Babin, A. Morel, and H. Claustre, "Variability in the chlorophyll-specific absorption coefficients of natural phytoplankton: analysis and parameterization," J. Geophys. Res. **100,** 13321–13332 (1995).
18. M. Kahru and B. G. Mitchell, "Spectral reflectance and absorption of a massive red tide off Southern California," J. Geophys. Res. **103,** 21601–21609 (1998).
19. A. Morel and S. Maritorena, "Bio-optical properties of oceanic waters: a reappraisal," J. Geophys. Res. **106,** 7163–7180 (2001).
20. H. Loisel and A. Morel, "Light scattering and chlorophyll concentration in Case 1 waters: a reexamination," Limnol. Oceanogr. **43,** 847–858 (1998).
21. G. Fournier and J. L. Forand, "Analytic phase functions for ocean water," in *Ocean Optics XII*, J. S. Jaffe, ed., Proc. SPIE **2258,** 194–201 (1994).
22. Z. Ahmad, J. R. Herman, A. Vasilkov, M. Tzortziou, B. G. Mitchell, and M. Kahru, "Seasonal variation of UV radiation in the ocean under clear cloudy conditions," in *Ultraviolet Ground- and Space-Based Measurements, Models, and Effects*, J. R. Slusser, J. R. Herman, and W. Gao, eds., Proc. SPIE **5156,** 63–73 (2003).
23. N. K. Hojerslev, "Optical properties of sea water," in *Landolt-Bornstein Numerical Data and Functional Relationships in Science and Technology*, J. Sundermann, ed. (Springer-Verlag, New York, 1986), pp. 263–281.
24. H. R. Gordon, "Can the Lambert–Beer law be applied to the diffuse attenuation coefficient of ocean water?" Limnol. Oceanogr. **34,** 1389–1409 (1989).
25. A. P. Vasilkov, J. Herman, Z. Ahmad, M. Kahru, B. G. Mitchell, and M. Tzortziou, "A comparison of UV penetration into ocean waters with models and *in situ* data," in *Proceedings of the Ocean Optics XVI Conference* (CD-ROM) (Office of Naval Research, Arlington, Va., 2002).
26. C. D. Mobley, L. K. Sundman, and E. Boss, "Phase function effects on oceanic light fields," Appl. Opt. **41,** 1035–1050 (2002).
27. A. P. Vasilkov, J. Herman, Z. Ahmad, M. Kahru, and G. Mitchell, "Model for the assessment of UV penetration into ocean waters from space-based measurements and full radiative transfer calculations," in *Ultraviolet Ground- and Space-Based Measurements, Models, and Effects III*, J. R. Slusser, J. R. Herman, and W. Gao, eds., Proc. SPIE **5156,** 316–322 (2003).